

An Integrated Thresholding and Morphological Process with Histogram-based Method for Brain Tumor Analysis and MRI Tumor Detection

A R Deepa¹, Mousmi Ajay Chaurasia^{2*}, Peram Sai Harsha Vardhan¹, Ganishetti Ritwika¹, Mamillapalli Samanth Kumar¹, Yaswanth Chowdary Nettm¹

¹Koneru Lakshmaih Education Foundation, Guntur, A.P

²Muffakham Jah College of Engineering & Technology, Hyderabad

Abstract

INTRODUCTION: Over the past several years analysis of image has moved from larger system to pervasive portable devices. For example, in pervasive biomedical systems like PACS-Picture archiving and Communication system, computing is the main element. Image processing application for biomedical diagnosis needs efficient and fast algorithms and architecture for their functionality. Future pervasive systems designed for biomedical application should provide computational efficiency and portability. The discrete wavelet transform (DWT) designed in on-chip been used in several applications like data, audio signal processing and machine learning.

OBJECTIVES: The conventional convolution based scheme is easy to implement but occupies more memory, power and delay. The conventional lifting based architecture has multiplier blocks which increase the critical delay. Designing the wavelet transform without multiplier is an effective task especially for the 2-D image analysis. Without multiplier Daubechies wavelet implementation in forward and inverse transforms may find efficient. The objective of the work is on obtaining low power and less delay architecture.

METHODS: The proposed lifting scheme for two dimensional architecture reduces critical path through multiplier less and provides low power, area and high throughput. The proposed multiplier is delay efficient.

RESULTS: The architecture is Multiplier less in the predict and update stage and the implementation carried out in FPGA by the use of Quartus II 9.1 and it is found that there is reduction in consumption of power at approximately 56%. There is reduction in delay due to multiplier less architecture.

CONCLUSION: multiplier less architecture provides less delay and low power. The power observed is in milliwatts and suitable for high speed application due to low critical path delay.

Keywords: Brain Tumor, Medical Image Processing, MRI images, grayscale images, Thresholding

Received on 18 December 2023, accepted on 16 March 2024, published on 21 March 2024

Copyright © 2024 A. R. Deepa *et al.*, licensed to EAI. This is an open access article distributed under the terms of the [Creative Commons Attribution license](#), which permits unlimited use, distribution and reproduction in any medium so long as the original work is properly cited.

doi: 10.4108/eetpht.10.5498

1. Introduction

MRI and CT scans are valuable tools for detecting brain tumors, using magnetic fields instead of x-rays to generate precise body images. The precise and reliable identification of brain tumors is of paramount importance. Enhancing accuracy can be accelerated through the utilization of a computer-aided system. This technology

empowers radiologists to identify brain tumors with heightened precision. Our research introduces an innovative computer-assisted approach designed to elevate the accuracy of brain tumor detection, as well as to determine tumor size and location. It also aids in assessing the malignancy of the tumor. Furthermore, neurologists must take into account factors such as the tumor's width, height, surface area, or thickness when making decisions about surgical intervention.

*Corresponding author. Email: mousmi.ksu@ieec.org

2. Literature Survey

In their study [2], Rohan Kandwal and colleagues primarily emphasized the importance of post-processing rather than focusing on brain tumor detection. Furthermore, this research did not provide information about the accuracy rate. In contrast, in [3], Jasdeep Kaur introduced a method aimed at enhancing the effectiveness of the weighted median filter and switching median filter in detecting and eliminating impulse noise from grayscale digital images.

In reference [4], Mr. Rohit S. Kabade has introduced an approach that expedites the analysis process while achieving tumor tissue segmentation with an accuracy and reproducibility level comparable to manual segmentation. Tumor segmentation poses several challenges, particularly the time-consuming manual detection process. In their work titled "An Efficient Brain Tumor Detection Algorithm Using Threshold & Threshold Based Segmentation" [5], Anam Mustaqeem, Ali Javed, and Tehseen Fatima proposed a method based on threshold segmentation, watershed segmentation, and morphological operators. However, the effectiveness of this method in actual practice remains uncertain. On the other hand, Swe Zin Oo and Aung Soe Khaing put forth an approach for tumor identification utilizing the morphological erosion algorithm in reference [6]. The primary drawback of this method is its limited success rate, operating effectively only 52.78% of the time, and exhibiting a notably low level of accuracy.

3. Background Methodology

The data was sourced from the BRATS brain cancer database, comprising four distinct image types (T1, T2, T1C, and FLAIR) for each patient. In our study, we specifically utilized the FLAIR images from a sample of 76 individuals. These images were originally stored as 3D files in the .mha format, and we converted them into 2D images in the .png format using the Look 3D software.

A. Histogram Method

In this method, the initial input image was initially converted to grayscale. Subsequently, a histogram equalization technique was applied to the grayscale image to enhance the contrast of image intensity, making it easier to identify the brightest regions within the image. Following this enhancement, the image underwent smoothing through median filtering. Prior to applying adaptive thresholding with an 'Otsu' threshold value of 0.31, certain nearly white pixels were adjusted to pure white, while others were transformed into darker pixels. Subsequently, the image was converted into a binary representation. Morphological operations were then implemented, involving both dilation and erosion, using a structural element of $[1;1;1]$. This step significantly improved the segmentation process, simplifying the accurate identification of tumor areas. Any regions containing fewer than 250 pixels were subsequently removed. Finally, the cancer site was pinpointed.

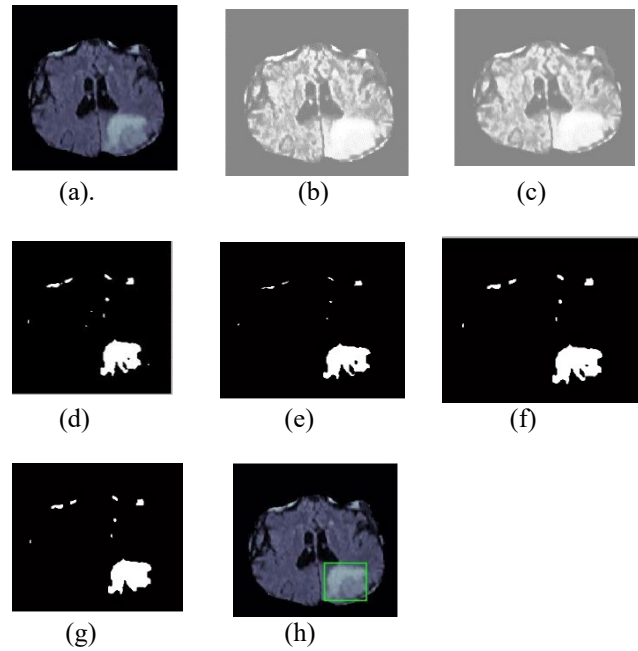


Fig 1: The following steps are used in the detection of tumours step by step: (a) input image; (b) histogram image; (c) after-medfiltering image; (d) binarization; (e) erosion; (f) dilation; (g) after-morphological hole filling; and (h) tumour detected image.

Using this technique, we have found the following outcomes:

- When the histogram was used, the image's general contrast significantly improved. As a consequence, some white pixels were added to less bright areas.
- Some white pixels that weren't supposed to be white showed up as we added more pixels. Problems arise when we split the affected area into linked, large white areas.
- Applying the filter reveals that the alleged connecting pixels disappear and, through morphological action, completely vanish. So that they wouldn't be lost during morphological operations, we made an attempt to restore those pixels.
- This problem caused us to misidentify the affected region.

Hence, we determined that this technique is less accurate based on the results.

B. Revised Integrated Thresholding and Morphological Method

This technique involved making grayscale copies of the FLAIR pictures first. For Otsu's approach, grayscale pictures are kept in a different variable.

We used the Basic Global Thresholding technique because it allows us to identify the regions of the brain that are most affected. First, a global cutoff number T is started. The image is divided into two groups using T : group 1 is made up of pixels with values higher than T , and group 2 is made up of pixels with values lower or equivalent to T . The two groups' average levels are used to calculate it. The average of the two mean intensity numbers is then used to determine a new threshold value.



Fig 2: Changing the size and location of the brain

We applied the average filtering technique to the images using the filter mask $[-1 \ 2 \ -1; 0 \ 0 \ 0; 1 \ -2 \ 1]$ from the 4 neighbourhood. 25 was added to the picture to improve it. Other than 25, no other numbers should be used because they would make the images too bright for proper segmentation.

Then, we applied the pictures with Otsu's global thresholding technique. It utilises two sets of pixel variations known as the foreground and backdrop.

Mean: It is determined by multiplying the total number of pixels in an area of interest by the sum of the pixel intensities. The equation is:

$$\text{Mean} = (1/N) * \sum(x_i)$$

where N represents the total number of pixels in the area and x_i represents the i -th pixel's intensity value.

Standard deviation: It is a measurement of how much the pixel intensities vary throughout an area of interest. It goes like this:

$$\text{Standard deviation} = \sqrt{(1/N) * \sum((x_i - \text{mean})^2)}$$

where N is the region's total number of pixels, x_i is the pixel's intensity value for position i , and mean is the region's average intensity value.

Entropy: It is a measurement of the texture's complexity or randomness in a certain area of an image. The equation is:

$$\text{Entropy} = - \sum(p_i * \log_2(p_i))$$

where p_i is the likelihood that a specific gray-level intensity value will be present in the area.

Contrast: The difference in pixel brightness between adjacent image regions is measured. It goes like this:

$$\text{Contrast} = \sum(i-j)^2 * p(i,j)$$

where $p(i,j)$ denotes the likelihood that i and j would occur together in the region, and i and j are neighbouring gray-level intensity values.

The class means and chances can be calculated using iterative methods. The best method to add 0.31 for better segmentation was to use the global threshold value. Best tumour area segmentation is provided. Except for 0.31, all other values between 0 and 1 are false. We choose 0.31 due to its better efficiency.

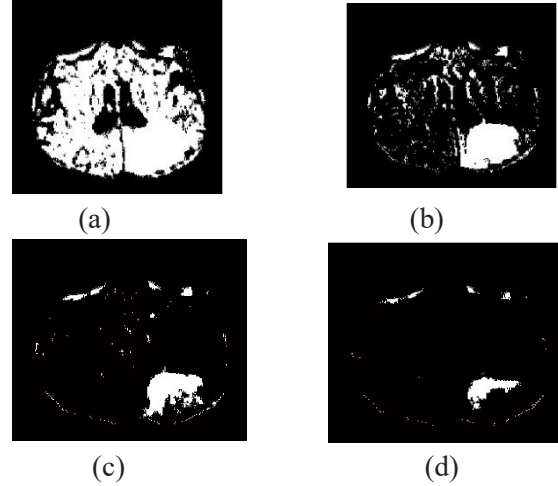


Fig 3: Using various Otsu' values during binarization

After that, `im2bw()` was used to transform the images to binary format.

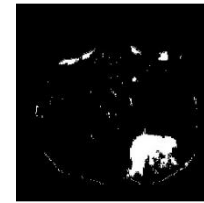


Fig 4: Binarization

The tumour has the highest pixel values in the image it has impacted. We connected the surrounding pixels that have a pixel value differential of less than 95 from the tumour pixels and joined the missing pixels of the picture we got after thresholding based on those pixel values. because there is a chance that a tumour could one day form from linked images. As a result, the missing pixels from the filtering process were restored. There might be a few empty spots. We have compared the current images with the ones that were previously stored in the variable in order to restore all of these pixels. As a result, every lost pixel was located.

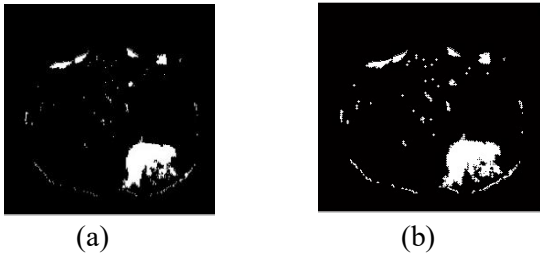


Fig 5: (A) Following the connection of adjacent pixels using the tumour pixel value; (B) following the connection of adjacent pixels using the global threshold image

$$\text{Ratio} = \frac{\text{Tumour area}}{\text{Brain area}} \times 100\%$$

The picture is divided into 4 smaller images, which are the image's four quadrants. The border pixels of each sub image are then determined. Among the subimages, we identify the tumour location with the most pixels. The tumour's region can then be determined based on where the largest portion of these subimages is located.

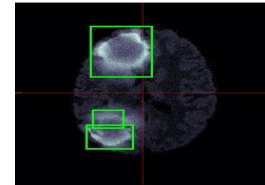


Fig 8: Location of Tumors

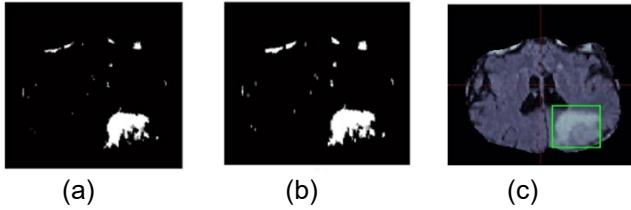


Fig 6: (a) Erosion of the morphology (b) dilation of the morphology (c) Detection of Tumor

There are two tumors present, and they constitute approximately 18.539% of the affected area. One of these tumors is situated in the lower left corner, with a tumor surface area of 0.946. A tumor is situated in the upper left corner, covering an area of 1.510. To determine the tumor's surface area, we can leverage the `imfinfo()` method, which provides details about the image. Of utmost importance are the "XResolution" and "YResolution" parameters, both expressed in terms of pixels per "ResolutionUnit," typically measured in "meter." With this information, we can calculate the image's pixel size as follows:

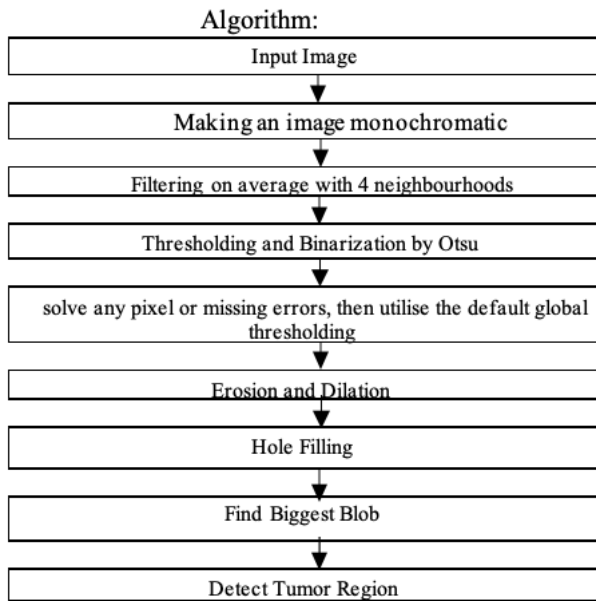


Fig 7: Revised Thresholding and Morphology Process Diagram

$$\text{PixelSize} = 1000 \quad \text{pixelsize} = 100 * (\text{YResolution} / \text{XResolution})$$

Once we have the pixel size in either millimeters per pixel or centimeters per pixel, we can calculate any area values by multiplying the number of non-zero pixels in the image (`nnz(bw5)`) by the pixel area, as shown in the formula:

$$\text{Area} = \text{nnz}(\text{bw5}) * \text{PixelSize}$$

This computation will yield the desired area measurement.

C. Number of Tumors

By connecting the tumour pixels to one another, we create a solid white blob. The `bwlabel()` function and the four neighbour approach can be used to calculate the number of cancers that are present in the brain. A patient rarely has two tumors, though.

D. Location and Affected Ratio of the Tumor

Similar to this method, we turn the tumour and the entire brain into white blobs and use the `nnz()` tool to calculate their areas. Then we can calculate their ratio using this formula:

4. Result Analysis

The proposed methodology was implemented on a computer equipped with an Intel Core i-5 processor running at a clock speed of 2.52 GHz. This method leverages MRI scans to precisely identify the locations of various brain tumors. The results of this approach successfully identified 66 out of 76 distinct images from individuals within the BRATS database. Consequently, the effective detection rate stands at 85.84%, surpassing the performance achieved by the previous TMP approach. The result is shown below:

Total FLAIR image : 76 Detected
Tumor : 66 Accuracy rate : 85.84%

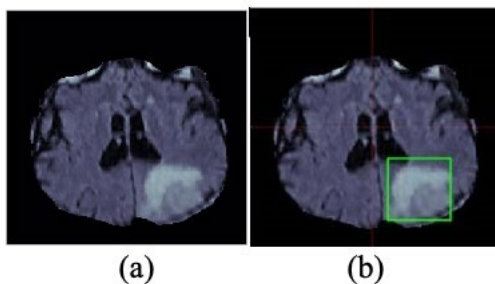


Fig 9: (a) FLAIR image input, (b) produced output picture

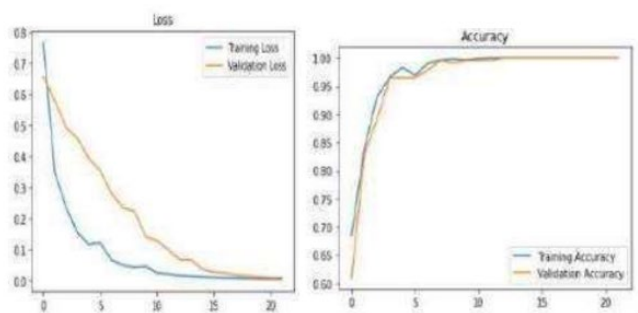


Fig 10: Accuracy graph and loss graph

Furthermore, we've prepared a chart that compares the detection success rates between the TMP technique and our proposed "Revised Integrated Thresholding and Morphological Process."

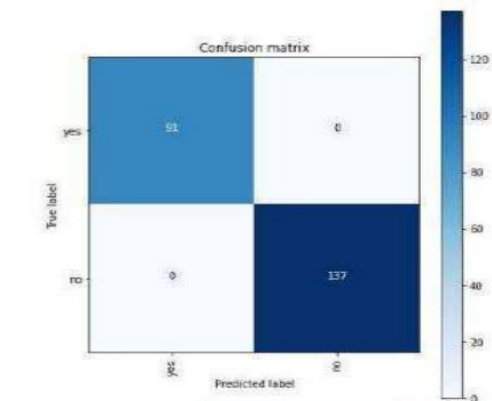


Fig 11: Accuracy comparison between Previous TMP method and Our Proposed method

For this purpose, we conducted a comparative analysis of our approach with methodologies employed by other authors using FLAIR images, achieving an accuracy rate of 85.84%. Based on the chart, we can confidently assert that this strategy holds significant promise.

Conclusion

The technique suggested in this study would be a very effective way to find brain tumours. In addition, the precision rate has improved in comparison to earlier studies. We have found that the method works very well for images that are especially clear and have less noise. In that regard, we assume that the accuracy rate would rise with the use of noise reduction and picture enhancement. In addition, it would be fantastic to create better techniques for detecting malignant brain tumours that are tiny in size. A significant accomplishment would occur if the real tumour size could be determined from the 3D image. Because doing so will aid in the planning of the tumour surgery by the physicians.

References

- [1] Pourasad, Y., Ranjbarzadeh, R. & Mardani, A. A new algorithm for digital image encryption based on chaos theory. *Entropy* 23(3), 341. <https://doi.org/10.3390/e23030341> (2021).
- [2] Ranjbarzadeh, R. & Saadi, S. B. Automated liver and tumor segmentation based on concave and convex points using fuzzy c-means and mean shift clustering. *Meas. J. Int. Meas. Confed.* <https://doi.org/10.1016/j.measurement.2019.107086> (2020).
- [3] AleedSalehi, A., Baglat, P. & Gupta, G. Review on machine and deep learning models for the detection and prediction of coronavirus. *Mater. Today Proc.* <https://doi.org/10.1016/j.matpr.2020.06.245> (2020).
- [4] Lei, B. et al. Self-co-attention neural network for anatomy segmentation in whole breast ultrasound. *Med. Image Anal.* 64, 101753. <https://doi.org/10.1016/j.media.2020.101753> (2020).
- [5] RRGCCAN: re-ranking via graph convolution channel attention network for person re-identification. *IEEE Access* 8, 131352–131360. <https://doi.org/10.1109/ACCESS.2020.3009653> (2020).
- [6] Ali, M. J. et al. Enhancing breast pectoral muscle segmentation performance by using skip connections in fully convolutional network. *Int. J. Imaging Syst. Technol.* <https://doi.org/10.1002/ima.22410> (2020).
- [7] Ranjbarzadeh, R. et al. Lung infection segmentation for COVID-19 Pneumonia based on a cascade convolutional network from CT images. *Biomed Res. Int.* <https://doi.org/10.1155/2021/5544742> (2021).